

Electron capture dynamics into self-assembled quantum dots far from equilibrium with their environment

L. Berg ¹, L. Schnorr,¹ J. Wilkens ¹, T. Heinzel ^{1,*}, C. Rothfuchs-Engels ², S. Scholz ², A. Ludwig,² and A. D. Wieck ²

¹*Solid State Physics Laboratory, Heinrich-Heine-Universität Düsseldorf, 40204 Düsseldorf, Germany*

²*Lehrstuhl für Angewandte Festkörperphysik, Ruhr-Universität Bochum, 44780 Bochum, Germany*



(Received 4 October 2023; revised 2 May 2024; accepted 7 June 2024; published 26 June 2024)

We report studies of the electron capture process in self-assembled quantum dots (SAQDs) far from equilibrium with their environment and at large distance to the reservoirs. Deep level transient spectroscopy is used to determine the capacitance transients in response to bias voltage pulses, from which the capture rates are obtained as a function of the temperature and the quantum dot occupancy. The observed activated character of the capture suggests that the dominant electron source is the back contact. A model is developed based on electrons diffusing from the reservoir across the flat band region and getting captured in the SAQDs after overcoming the barrier formed by the space charge region between its onset and the quantum dots. For small barriers, we identify a distinct tunneling contribution to the capture current.

DOI: [10.1103/PhysRevB.109.235433](https://doi.org/10.1103/PhysRevB.109.235433)

I. INTRODUCTION

Self-assembled quantum dots (SAQDs) are quasi-zero-dimensional semiconductor islands embedded in a host crystal with a larger band gap [1,2]. They can be considered as artificial atoms which can be ionized but also excited internally. This enables a wide variety of fundamental experiments [3–6] and technological applications [7]. In several implementations like quantum dot lasers [8,9] or light-emitting diodes [10], the SAQDs are positioned inside an extended, weakly conductive spacer layer that inhibits charge transfers close to equilibrium conditions. However, it is quite common to apply large electric fields to such structures, for example, in electrically driven single-photon sources or in floating-gate type storage devices [11]. Frequently, the capture process plays a crucial functional role. In single-photon sources as well as in storage devices, a short capture time is beneficial due to its influence on the repetition rates. A comprehensive understanding of the capture process is therefore of vital interest, not only for fundamental reasons, but also to optimize it according to the specific requirements. Hitherto, however, the electron capture under such conditions has not been studied thoroughly.

Here, we use deep level transient spectroscopy (DLTS) [12] to measure the capacitive capture transients as a function of the bias voltage and the temperature and discuss the underlying physics within a diffusive model based on band structure calculations. The work is complementary to previous studies on similar samples with focus on the emission process [13–25]. Capacitive capture transients on a similar sample have been reported before, however, without analysis or modeling of the data [24].

In Sec. II, the samples and experimental methods are described. Section III reports the DLTS measurements and the dependence of the measured time constant on temperature and

bias voltage. In Sec. IV, a model for the dominant capture process is proposed and alternative processes are discussed. The text concludes with a summary and an outlook (Sec. V).

II. EXPERIMENTAL SETUP AND MEASUREMENT TECHNIQUE

The layout of the sample and its preparation have been described in detail elsewhere [23–25]. In brief, we focus on InAs quantum dots embedded in a Ga[Al]As heterostructure as a model system. The structure is prepared by molecular beam epitaxy, with an SAQD layer 500 nm above a Si⁺ doped back contact and 413 nm below the sample surface; see Fig. 1(a). The SAQDs have a sheet density of $n_{QD} = 10^{14} \text{ m}^{-2}$. They are embedded in a 26 nm layer of undoped GaAs in order to avoid mutual influences of the dopants and the SAQD growth. Bias voltages can be applied to a Cr/Au top electrode with respect to the grounded back contact, which is accessed via a local region where In has been alloyed into the heterostructure. The gated area amounts to $A = (0.3 \text{ mm})^2$, covering approximately 9×10^6 quantum dots.

The measurements are taken in a liquid helium cryostat (Leiden Cryogenics), operated at temperatures between 3 K and 77 K. The sample rests in vacuum. The system is equipped with a superconducting solenoid, which allows the generation of magnetic fields up to $B = 11 \text{ T}$, oriented perpendicularly to the sample surface. Rectangular voltage pulses with levels for preparation (V_p) and measurement (V_m) of the SAQD occupancy are applied to the top gate with respect to the back contact, which is kept at virtual ground via a HF2TA transimpedance amplifier ($Z = 1 \text{ k}\Omega$) from Zurich Instruments. Its output is recorded with a 5444B digital oscilloscope (PicoTechnology) plus a HF2LI lock-in amplifier (Zurich Instruments), which also provides the ac voltage. The voltage pulses are generated using a Keithley Model 3390 arbitrary waveform generator with a transition time of 100 ns and

*Contact author: thomas.heinzel@hhu.de

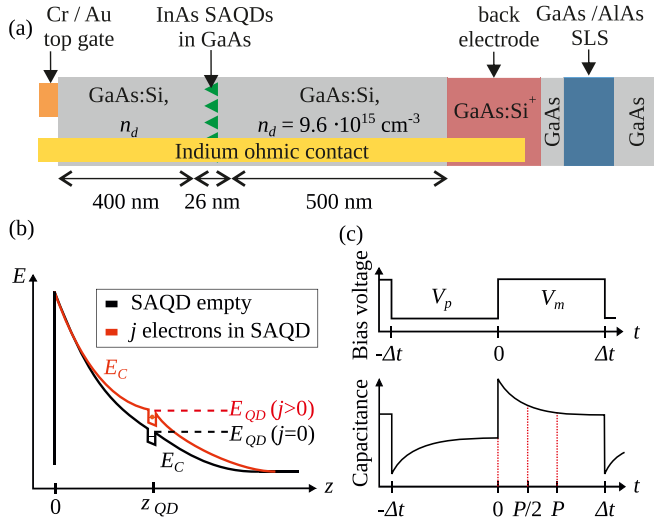


FIG. 1. (a) Cross sectional schematic view of the sample layout. The SAQD layer is indicated by the green triangles. The back electrode is accessed via an alloyed In contact and the top gate is formed by a Cr/Au electrode. The silicon doping density in the spacer layer is indicated by n_d . (b) Schematic band diagram for the case of a negative voltage applied to the top gate with respect to the grounded back electrode and its dependence on the SAQD occupation. (c) Schematic capacitance transients in response to rectangular bias voltage pulses (voltage levels V_p and V_m for the preparation and the measurement of the charge configuration, respectively) of duration Δt . The time window selected for the analysis is denoted by P .

superimposed with the ac voltage. In this setup, the output current obtained at a phase shift of $\pi/2$ with respect to the input ac voltage detects the differential capacitance of the sample. The excitation frequency of 28 MHz (amplitude 10 mV) was selected as a compromise between high time resolution and negligible dielectric relaxation.

III. LOCK-IN DLTS MEASUREMENTS

The initial state of the sample is prepared by applying a bias voltage V_p for a duration of $\Delta t = 491$ ms to the top gate with respect to the grounded back electrode. Afterwards, the measurement voltage V_m is applied for Δt and the capacitance transient is recorded with a time resolution of 10 μ s. In Fig. 1(c), the typical capacitive response of the sample to such bias voltage pulses is illustrated schematically. As the SAQDs are gradually filled with electrons, the (positive) charge density decreases locally, which is compensated by an increase of the depletion length, thereby leading to a decrease of the capacitance over time, which represents our primary measurement signal.

Lock-in DLTS [26] is very convenient for characterizing the charge transfer processes as a function of the temperature, the initial conditions, and of the applied voltage. Within this concept, the measured capacitance transients $C(t, V_p, V_m)$ are processed numerically according to

$$S(T, P, V_p, V_m) = \frac{1}{N_p} \left(\sum_{i=1}^{N_p/2} C_i - \sum_{i=N_p/2+1}^{N_p} C_i \right), \quad (1)$$

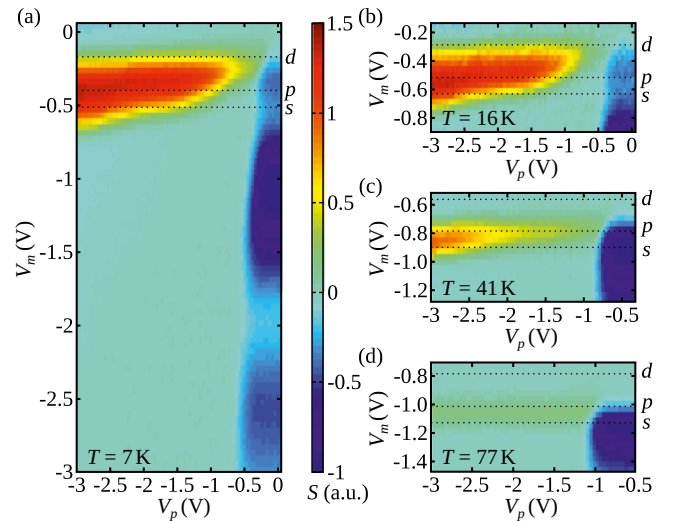


FIG. 2. Color plots of the measured lock-in DLTS signals $S(V_p, V_m)$ for various temperatures. The underlying experimental data are the same as those evaluated in Fig. 3 of Ref. [25]. The dotted horizontal lines denote the computed onset voltages for capture into previously empty s , p , and d states, respectively. The color bar, valid for all subfigures, represents the value of S in arbitrary units.

where T denotes the temperature and N_p is the number of data points (labeled by i) within the selected time window. In the case that the absolute value of $S(P)$ has a maximum, it appears at $P = \tau/0.398$, where τ is the time constant of an exponential transient. Furthermore, positive values of S indicate electron capture, while for negative S electrons are emitted from the SAQDs. With our setup, DLTS signals can be obtained for time windows P ranging from ≈ 100 μ s to Δt and P was selected according to the best visibility of the capture process.

In Fig. 2, the measured lock-in DLTS signals are reproduced for four different temperatures with focus on the voltage regime where capture is observed (i.e., $S > 0$). In these measurements, $P = 491$ ms has been used. For a temperature of 7 K shown in Fig. 2(a), the emission transients are located at $V_p \geq -0.7$ V and extend over the range $-3 \text{ V} \leq V_m \leq 0 \text{ V}$. They have been described in detail elsewhere [24,25] and will not be discussed here. We first focus on the capture behavior observed at $T = 7$ K; see Fig. 2(a). As the measurement voltage is increased starting from $V_m - 3$ V, capture sets in at $V_m \approx -650$ mV for a preparation voltage $V_p = -3$ V. As V_p is increased, this onset voltage increases as well in the form of two weakly pronounced steps. As V_m is further increased, the capture signal disappears abruptly and almost independently of V_p at $V_m = -200$ mV. A temperature increase, see Figs. 2(b)–2(d), causes the capture peak to shift towards lower V_m , reaching a value of $V_m = -1.05$ V at 77 K. This goes along with $S(V_m)$ becoming more symmetric, while the fine structure is suppressed and no longer visible at 77 K.

These observations can be interpreted qualitatively in a straightforward way. After applying a sufficiently negative preparation voltage pulse, the SAQDs are empty. As V_m is increased, the energies of the SAQD states with respect to the grounded back electrode decrease, thereby increasing the capture rate. At the lower edge of the peak, the time constant

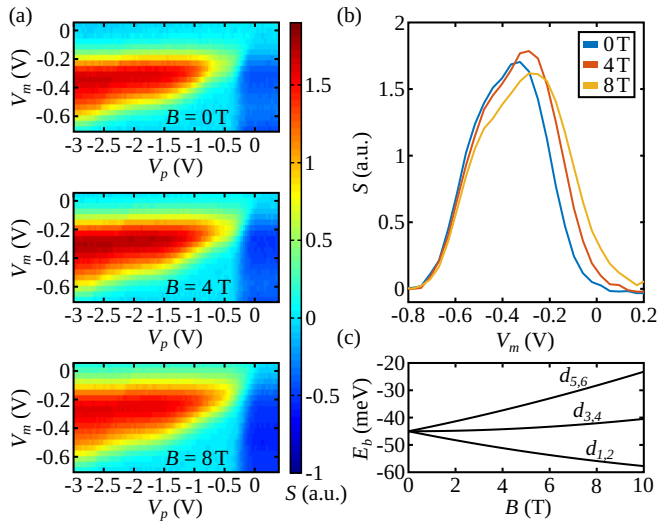


FIG. 3. Dependence of the lock-in signal on perpendicular magnetic fields B . (a) Evolution of $S(V_p, V_m)$ as B is increased and (b) lineouts $S(V_m, V_p = -3 \text{ V})$ thereof. Further functions $S(V_p, V_m)$ at different B are shown in the Supplemental Material. (c) Model calculation for the evolution of the binding energy E_B of the d states of the SAQDs as a function of B within the Fock-Darwin spectrum. Not shown is the splitting of the levels of the single electron charging energy of 15 meV per electron that enters an SAQD.

of the transient drops into the time window defined by the selection of P . Capture can be observed up to the measurement voltage where it becomes too fast to be measured with the selected $P - V_m = -200 \text{ mV}$ in the present case. For larger V_p values, the initial occupancy of the SAQDs increases, leading to a reduced capture signal, as well as to steps in the onset value of V_m when the SAQD states have remained occupied during the preparation stage. Furthermore, the temperature dependence implies a thermally activated capture process. As the temperature is increased, the average kinetic energy of the electrons to be captured increases as well, thus enabling capture with the same rate at larger SAQD energies. The substructure of the capture peak is suppressed under increasing temperature. For example, at 77 K and for negative bias voltages, the emission time constant for the p states can be estimated to 100 ns—two orders of magnitude below our resolution limit.

Apparently, despite the presence of strong electric fields, the capture comprises a dominant thermally activated process. This is not self-evident considering that the electrons could originate from, for example, the leakage current or field ionization of deep donors.

A perpendicular magnetic field B allows one to tune the SAQD energy levels independent of the applied electric field. The B dependence of the capture is summarized in Fig. 3(a). Cross sections of $S(V_m)$ at fixed V_p [selected in 3(b) was $V_p = -3 \text{ V}$] illustrate the composite structure of the S peak, comprising a B -independent component at lower V_m and a B -dependent contribution located at larger V_m values, i.e., for $V_m < \approx -500 \text{ mV}$, whose time constant increases with increasing magnetic field.

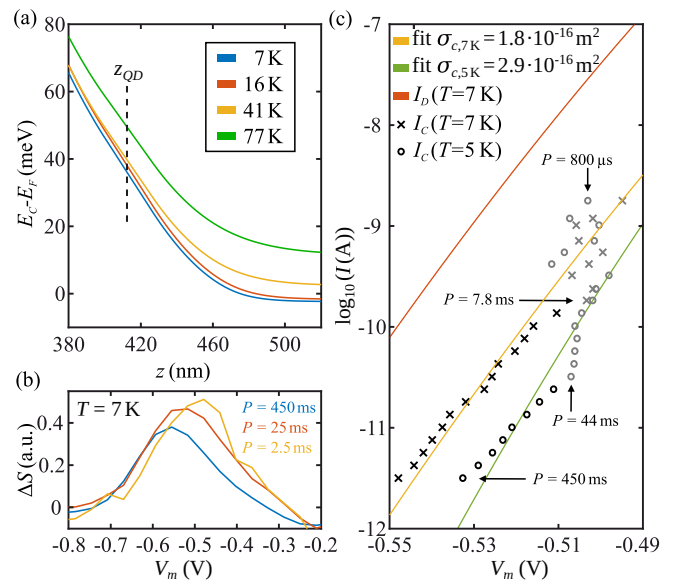


FIG. 4. (a) Calculated conduction band profiles for different temperatures at a bias voltage of -0.8 V . (b) Contribution ΔS to S from the SAQD s states for different time constants, as found for $T = 7 \text{ K}$ after subtracting the contributions from the p and d levels. (c) Current due to charging of the s states as a function of the measurement voltage for various time constants and for two temperatures $T = 5 \text{ K}$ (open circles) and 7 K (crosses) and the corresponding fits according to Eq. (4) with the capture cross section as fit parameter (green and yellow full lines). Also shown is the total diffusion current reaching z_{QD} (orange line). Only the black symbols have been used in the fits described in the text.

IV. MODEL FOR THE ELECTRON CAPTURE PROCESS

In this section, we are going to argue that, at large SAQD energies E_{QD} (low V_m), electrons get captured predominantly from the diffusion current arriving at the SAQD site from the back electrode. At lower E_{QD} , the barrier between the back electrode and the SAQD is sufficiently small to allow additional tunneling between the conduction band and the d states of the SAQDs.

To identify the origin of the captured electrons, we first compute the conduction band profile. The doping density in the spacer layer is obtained from capacitance-voltage measurements followed by a Mott-Schottky analysis to $n_d = 9.6 \times 10^{15} \text{ cm}^{-3}$ and a built-in potential barrier of $V_{bi} = 650 \text{ mV}$ is extracted [27]. These values are used as input for one-dimensional, self-consistent Poisson-Schrödinger calculations of the conduction band profile [28]. Here, the SAQD layer is included in the form of a two-dimensional charge layer, with an electron density that corresponds to the assumed occupancy of the SAQDs. Literature values for the temperature dependent dielectric constant of GaAs have been used [29]. It becomes apparent that the capture by initially empty dots sets in at measurement voltages where the SAQD layer resides close to, i.e., within $\approx 50 \text{ nm}$ of the edge of the space charge region. At these conditions, the barrier height with respect to the Fermi level of the back electrode is relatively small; see Fig. 4(a) for an example. As the temperature is increased from 7 K to 77 K, E_{QD} increases by $\approx 20 \text{ meV}$.

Now, thermally activated electrons can diffuse from the back electrode across the flat band region into the space charge layer and may get captured in SAQD states. For this process, the capture rate equals the flux density of diffusing electrons at the location z_{QD} of the SAQDs, multiplied by the capture cross section σ_c [30]. Comparing this situation at $V_m = -0.8$ V, for example, to the measured capture signal with $\tau = 195$ ms as shown in Fig. 2, this effective barrier between the back contact and the SAQDs is too large for capture at 7 K and 16 K, while at 41 K a peak in S is observed. As T is increased further to 77 K, the capture time drops well below 195 ms and the lock-in DLTS signal vanishes.

For an initial nonzero occupancy, the Coulomb interaction increases the energy barrier of height $E(z_{QD}, V_m, k)$, where k denotes the number of electrons in one dot at the end of the preparation pulse. Therefore, the capture of additional electrons per SAQD sets in at a steplike increasing value for V_m as the preparation voltage increases, in agreement with the observations. Since $E(z_{QD})$ increases with the occupancy, the onset value for V_m at which filling of a particular level starts can be estimated with the Poisson Schrödinger solver for each occupancy at a given value for V_p , by calculating the detectable diffusion current according to Eq. (3). In Fig. 2, the computed values for V_m required to fill the first, the third, and the seventh electron (i.e., the onset of filling electrons in the s , p , and d levels, respectively) in the SAQDs are included as dashed horizontal lines. These values agree reasonably well with the observed fine structure of the capture peak.

We now focus on the filling of the s states after a preparation voltage of $V_p = -3$ V, assuming that the electrons can enter the SAQDs via all their energy levels and then relax rapidly into the s states. The contribution of the s state filling to the capture signal is isolated by subtracting $S(V_m)$ for $V_p = -2$ V (where capture into the s state is negligible) from the function $S(V_m)$ measured at $V_p = -3$ V.

The time constants $\tau(V_m, T)$ follow directly from the measured transients and reflect the effective time of charge transfer between the SAQDs and the environment, composed of both capture and emission of electrons. It can be interpreted directly as capture time constant τ_c only in limiting cases where emission is negligible. This is certainly not justified at higher temperatures or over the full interval of bias voltages. For example, in the measurement at $T = 7$ K close to $V_p = V_m = -0.5$ V, Fig. 2(a), S vanishes, indicating that the two transfer rates are identical. Previously, a rate equation model has been established which allows the separation of the capture and emission rates [25]. It shows that, after our preparation time interval, all SAQD states are empty for $V_p \lesssim -2.8$ V, since $\tau_e \ll P \ll \tau_c$, where τ_e denotes the emission time constant. The difference $\Delta S(V_m) \equiv S(V_m, V_p = -3$ V) $- S(V_m, V_p = -2$ V) therefore represents the capture solely into the s states and is shown in Fig. 4(b) for a few exemplifying rate windows. The maximum of $\Delta S(V_m)$ shifts to larger voltages as the selected time window P is decreased, reflecting the faster charging under more positive bias voltages. The corresponding charging current I_c during capture can be estimated by

$$I_c(V_m) = A \frac{en_{QD}}{\tau(V_m)}, \quad (2)$$

where e denotes the elementary charge. These values, with the time constant obtained from the maximum of a Gaussian function fitted to $\Delta S(V_m)$, are plotted in Fig. 4(c) for two temperatures. Apparently, at $T = 5$ K, the charging current increases approximately exponentially with V_m , with an abrupt increase of the exponent at $V_m \approx -0.505$ V, suggesting that the charging mechanism changes for sufficiently low potential barriers. As the temperature is increased to $T = 7$ K, I_c is larger for the same measurement voltage, with a comparable exponent. However, a kink at larger V_m is no longer clearly visible. Rather, the extracted values for I_c become quite noisy for $V_m \geq -0.51$ V, a consequence of the small P values.

The measured current can be compared to the calculated diffusion current $I_D(V_m)$ generated by electrons arriving at z_{QD} from the back electrode,

$$I_D(V_m) = eA \times \mu k_B T \frac{dn}{dz}. \quad (3)$$

Here, the density and the mobility of the electrons are denoted by n and μ , respectively, and the SAQDs are assumed to be empty initially. The diffusion current $I_D(V_m)$ obtained for $V_m \leq -0.505$ V and $V_m \leq -0.51$ V for $T = 5$ K and $T = 7$ K, respectively, has the same shape as the capture current $I_c(V_m)$; see Fig. 4(c). These currents are related by

$$I_c(V_m) = I_D(V_m)n_{QD} \times \sigma_c. \quad (4)$$

A least squares fit according to Eq. (4) is carried out for data at $T = 5$ K in the interval $V_m < -0.505$ V, using σ_c as a fit parameter that takes the value $\sigma_c = 1.8 \times 10^{-16}$ m², which is plausible considering that the SAQDs have an approximately conical shape with a base radius of ≈ 15 nm [31]. This analysis has been carried out for the other temperatures as well, which gives similar capture cross sections within a factor of 2 [27]. The case of $T = 7$ K thereof has been included in Fig. 4(c).

For the lowermost temperature and $V_m \geq -0.505$ V, the exponent of $I_c(V_m)$ shows a different slope. In this regime, the barrier between the flat band region and the SAQDs is of the order of a few meV only and decreases with increasing V_m . Thus tunneling through this barrier becomes possible and may contribute to the capture current. As V_m is increased, both the thickness and the height of the barrier decrease, while the spectral electron density around E_{QD} increases. It appears plausible that as a result a strongly gate voltage-dependent tunnel current evolves, which may be composed of elastic and thermally activated components. Due to its dependence on several parameters, modeling the tunneling current in this system is not very trustworthy with the information at hand and we therefore refrain from a quantitative description. Since, however, the barrier for tunneling into the s , p , and d states is very large, capture by tunneling under these conditions is expected to take place via high lying states only, which are no longer bound in occupied dots.

In view of this analysis, the B -independent lower edge of $S(V_m)$ in Figs. 3(a) and 3(b) can be interpreted as a diffusion-dominated regime. The upper, B -dependent tails of these peaks are dominated by tunneling into the d states of the SAQDs with occupied s and p levels: as B increases, the levels d_3 – d_6 , see Fig. 3(c), increase in energy and thus the spectral density of electrons available for tunneling decreases, which results in larger capture time constants. This line of

arguing is similar to that one used to explain the magnetic field dependence of the emission by tunneling, as observed with conventional DLTS [19]. The full spectra $S(V_m, V_p)$ as a function of B as well as lineouts in the emission-dominated regime are represented and interpreted in Fig. 4 of the Supplemental Material [27].

We conclude this section with three remarks. First of all, the leakage current is below our resolution limit in the studied bias voltage interval [27]. It therefore does not contribute significantly to the filling of the SAQDs. Second, the energy resolution of the measurement concept used here is too low to observe the effects of single electron charging on the capture dynamics within one orbital energy level. In the diffusion-dominated capture regime, the time constant changes rapidly with V_m and generates a narrow peak in $S(V_m)$. In the capture regime dominated by tunneling, on the other hand, the capture time constants are too close to our resolution limit. Possibly, the resolution can be improved by applying the much more time-consuming Laplace transform spectroscopy, where the single electron charging energy could be well resolved during emission processes [23]. Finally, the shape of the capture peak in the (V_p, V_m) plane can be modeled by solving the system of rate equations with $c_k(V_p, V_m)$ as a fit parameter, where the c_j represent the capture rates into level j . However, these complements do not contribute to the identification of the capture process and are beyond the scope of the present work.

V. SUMMARY AND CONCLUSIONS

We have used capacitive deep level transient spectroscopy to characterize the electron capture into self-assembled quantum dots which are far from equilibrium with their environment and reside at a large distance from the reservoirs.

The measured time constants of the transients contain, but are not equal to, the capture time, since significant emission takes place during capture over a wide parameter range. Therefore, the capture process has been analyzed in the voltage regime where emission is negligible. The capture shows a predominantly activated behavior. The combination of the experiments with Poisson-Schrödinger simulations suggest that, after changing the band structure by a bias voltage step, a new steady state will be established by a diffusion current $\propto dn/dz$, which fills the SAQDs up to the local quasi-Fermi level. Capture occurs predominantly if the SAQD layer is sufficiently close to the edge of the space charge region, such that the remaining barrier can be overcome thermally. Since under these assumptions the capture current as obtained from the capacitance transients should equal the diffusion current, the capture cross section of the s states can be estimated to $\sigma_c \approx 3 \times 10^{-16} \text{ m}^2$. For sufficiently small energy barriers between the SAQDs and the flat band region, tunneling contributes to the capture as well and we have explained the magnetic field dependence of the capture rates by tunneling into d states or, in the case of empty dots, into higher states. Future work may comprise measurements at higher energy resolution, for example, by using Laplace transform spectroscopy, with the possible identification of spin-selective charging as well as further capture mechanisms. Also, a detailed modeling of the capture peak with voltage-dependent capture rates, based on a rate equation model, is a possible next step.

ACKNOWLEDGMENTS

C.R.-E., S.S., A.D.W., and A.L. gratefully acknowledge the support of TRR 160/2-Project No. B04, Deutsche Forschungsgemeinschaft Grant No. 383065199, and the Deutsch-Französische Hochschule Grant No. CDFA-05-06.

-
- [1] D. Leonard, M. Krishnamurthy, C. M. Reaves, S. P. Denbaars, and P. M. Petroff, Direct formation of quantum-sized dots from uniform coherent islands of In[Ga]As on GaAs surfaces, *Appl. Phys. Lett.* **63**, 3203 (1993).
 - [2] P. M. Petroff, A. Lorke, and A. Imamoglu, Epitaxially self-assembled quantum dots, *Phys. Today* **54**(5), 46 (2001).
 - [3] P. Michler, A. Kiraz, C. Becher, W. V. Schoenfeld, P. M. Petroff, L. Zhang, E. Hu, and A. Imamoglu, A quantum dot single-photon turnstile device, *Science* **290**, 2282 (2000).
 - [4] M. Kroutvar, Y. Ducommun, D. Heiss, M. Bichler, D. Schuh, G. Abstreiter, and J. J. Finley, Optically programmable electron spin memory using semiconductor quantum dots, *Nature (London)* **432**, 81 (2004).
 - [5] C. L. Salter, R. M. Stevenson, I. Farrer, C. Nicoll, D. A. Ritchie, and A. J. Shields, An entangled-light-emitting diode, *Nature (London)* **465**, 594 (2010).
 - [6] A. Faraon, A. Majumdar, D. Englund, E. Kim, M. Bajcsy, and J. Vuckovic, Integrated quantum optical networks based on quantum dots and photonic crystals, *New J. Phys.* **13**, 055025 (2011).
 - [7] D. J. Mowbray and M. S. Skolnick, New physics and devices based on self-assembled semiconductor quantum dots, *J. Phys. D: Appl. Phys.* **38**, 2059 (2005).
 - [8] V. M. Ustinov, N. A. Maleev, A. E. Zhukov, A. R. Kovsh, A. Y. Egorov, A. V. Lunev, B. V. Volovik, I. L. Krestnikov, Y. G. Musikhin, N. A. Bert, P. S. Kopev, and Z. I. Alferov, InAs/InGaAs quantum dot structures on GaAs substrates emitting at 1.3 μm , *Appl. Phys. Lett.* **74**, 2815 (1999).
 - [9] E. U. Rafailov, M. A. Cataluna, and W. Sibbett, Mode-locked quantum-dot lasers, *Nat. Photon.* **1**, 395 (2007).
 - [10] I. L. Krestnikov, N. A. Maleev, A. V. Sakharov, A. R. Kovsh, A. E. Zhukov, A. F. Tsatsulnikov, V. M. Ustinov, Z. I. Alferov, N. N. Ledentsov, D. Bimberg, and J. A. Lott, 1.3 μm resonant-cavity InGaAs/GaAs quantum dot light-emitting devices, *Semicond. Sci. Technol.* **16**, 844 (2001).
 - [11] T. Nowozin, A. Marent, M. Geller, D. Bimberg, N. Akcay, and N. Öncan, Temperature and electric field dependence of the carrier emission processes in a quantum dot-based memory structure, *Appl. Phys. Lett.* **94**, 042108 (2009).
 - [12] D. V. Lang, Deep-level transient spectroscopy: A new method to characterize traps in semiconductors, *J. Appl. Phys.* **45**, 3023 (1974).
 - [13] S. Anand, N. Carlsson, M.-E. Pistol, L. Samuelson, and W. Seiffert, Deep level transient spectroscopy of InP quantum dots, *Appl. Phys. Lett.* **67**, 3016 (1995).

- [14] C. M. A. Kapteyn, F. Heinrichsdorff, O. Stier, R. Heitz, M. Grundmann, N. D. Zakharov, D. Bimberg, and P. Werner, Electron escape from InAs quantum dots, *Phys. Rev. B* **60**, 14265 (1999).
- [15] S. W. Lin, C. Balocco, M. Missous, A. R. Peaker, and A. M. Song, Coexistence of deep levels with optically active inas quantum dots, *Phys. Rev. B* **72**, 165302 (2005).
- [16] S. Schulz, A. Schramm, C. Heyn, and W. Hansen, Tunneling emission from self-assembled inas quantum dots probed with capacitance transients, *Phys. Rev. B* **74**, 033311 (2006).
- [17] M. Geller, E. Stock, C. Kapteyn, R. L. Sellin, and D. Bimberg, Tunneling emission from self - organized InGaAs/GaAs quantum dots observed via time - resolved capacitance measurements, *Phys. Rev. B* **73**, 205331 (2006).
- [18] O. Engström, M. Kaniewska, M. Kaczmarczyk, and W. Jung, Electron tunneling from quantum dots characterized by deep level transient spectroscopy, *Appl. Phys. Lett.* **91**, 133117 (2007).
- [19] A. Schramm, S. Schulz, J. Schäfer, T. Zander, C. Heyn, and W. Hansen, Electron emission from self-assembled quantum dots in strong magnetic fields, *Appl. Phys. Lett.* **88**, 213107 (2006).
- [20] A. Schramm, S. Schulz, C. Heyn, and W. Hansen, Suppression of competing tunneling processes in thermally-activated carrier emission on self-assembled InAs quantum dots, *Phys. Rev. B* **77**, 153308 (2008).
- [21] A. Schramm, S. Schulz, T. Zander, C. Heyn, and W. Hansen, Thermionic tunneling through coulomb barriers in charged self-assembled quantum dots, *Phys. Rev. B* **80**, 155316 (2009).
- [22] T. Nowozin, L. Bonato, A. Högner, A. Wiengarten, D. Bimberg, W.-H. Lin, S.-Y. Lin, C. J. Reyner, B. L. Liang, and D. L. Huffaker, 800 meV localization energy in GaSb/GaAs/Al_{0.3}Ga_{0.7}As quantum dots, *Appl. Phys. Lett.* **102**, 052115 (2013).
- [23] L. Schnorr, T. Heinzel, S. Scholz, A. Ludwig, and A. D. Wieck, Laplace deep level transient spectroscopy on self-assembled quantum dots, *J. Appl. Phys.* **124**, 104301 (2018).
- [24] L. Schnorr, J. Labes, L. Kurten, T. Heinzel, C. Rothfuchs-Engels, S. Scholz, A. Ludwig, and A. D. Wieck, Electron capture and emission dynamics of self-assembled quantum dots far from equilibrium with the environment, *Phys. Rev. B* **104**, 035303 (2021).
- [25] L. Schnorr, O. Khoukhi, L. Berg, T. Heinzel, C. Rothfuchs-Engels, S. Scholz, A. Ludwig, and A. D. Wieck, Hysteretic capacitance-voltage characteristics of self-assembled quantum dots far from equilibrium with their environment, *Phys. Rev. B* **104**, 205310 (2021).
- [26] G. L. Miller, D. V. Lang, and L. C. Kimerling, Capacitance transient spectroscopy, *Annu. Rev. Mater. Sci.* **7**, 377 (1977).
- [27] See Supplemental Material at <http://link.aps.org/supplemental/10.1103/PhysRevB.109.235433> for characterization measurements and the capture analysis at additional temperatures as well as in further magnetic fields.
- [28] G. Snider, *1D Poisson-Schrödinger solver* [accessed on Sep 15, 2017].
- [29] I. Strzalkowski, S. Joshi, and C. R. Crowell, Dielectric constant and its temperature dependence for GaAs, CdTe, and ZnSe, *Appl. Phys. Lett.* **28**, 350 (1976).
- [30] P. Blood and J. Orton, in *The Electrical Characterization of Semiconductors: Majority Carriers and Electron States*, edited by N. H. March (Academic Press, New York, 1992).
- [31] L. Schnorr, Electron capture and emission dynamics of self-assembled quantum dots, Ph.D. thesis, HHU Düsseldorf, 2022.